Journal of Mining and Earth Sciences
Website: http://jmes.humg.edu.vn

Highly photocatalytic activity of natural halloysite - based material for the treatment of dyes in wastewater

Son Ha Ngo*, Nui Xuan Pham, Tuan Ngoc Tran

Hanoi University of Mining and Geology, Hanoi, Vietnam

ARTICLE INFO

Article history:
Received 19th Dec. 2020
Revised 17th Apr. 2021
Accepted 15th May 2021

Keywords:
Ag - TiO_2,
Halloysite,
Photocatalyst,
RR - 195,
TiO_2.

ABSTRACT

In this study, the halloysite nanotube material will be fabricated from a natural halloysite mineral and used as a support for the photocatalytic activity phase based on TiO_2. The material is characterized by modern physicochemical methods such as XRD, SEM, BET, UV - vis spectrum, and EDX. Accordingly, the refined halloysite has a nanoscale with a length of about 1.3 µm and a capillary size of about 5 nm. After the deposition of Ag - TiO_2 on the halloysite, the specific surface of the material measured by the BET method was about 60 m^2/g, and the structure of the halloysite was intact. The band - gap energy of as - prepared materials is also significantly improved in comparison to pure TiO_2, makes the material capable of absorbing longer wavelengths of light in the photocatalytic process. The Photocatalyst based on Halloysite and TiO_2 showed very high efficiency, up to more than 95% in the decomposition of typical organic pollutant RR - 195. This result shows great potential in this novel material in environmental treatment applications.

1. Introduction

Reactive dyes are one of the most important technological advances of the 20th century in the field of textile. They are used more and more because they have bright colours, rich varieties, and high colour fastness. Currently, the number of reactive dyes in the textile industry accounts for about 50% of the total amount of dyes used on the market. However, the use of dye also leads to environmental problems such as residual dyeing compounds and chemical additives used in the dyeing process in wastewater (Bagane et al., 2000). These wastes are dangerous to the environment, especially aquatic habitats, if not being treated thoroughly (Imamura et al., 2002) due to its solubility in water and stability in this environment even with low concentrations. Therefore, the removal of dyes has received the huge attention of researchers.

*Corresponding author
E - mail: ngohason@humg.edu.vn
DOI: 10.46326/JMES.2021.62(3).03

Adsorption using activated carbon has long been used to remove various pollutants in water. However, adsorption is only the first step to collect pollutants and cannot treat them completely. Therefore, many scientists have studied the feasibility of using inexpensive, commercially available materials as dye removal agents by highly efficient processes without secondary pollutant generation.

Recently, natural halloysite has been attracted far - reaching interest for effective water treatment. This is a low - priced and abundant material with numerous advantages such as good dispersibility, rich in active groups, low toxicity, good biological compatibility and availability in nature (Zhang et al., 2016).

In the field of photocatalysis for environmental treatment, the most popular nanomaterial is TiO_2 nanoparticles. TiO_2 is a non - toxic material which has been applied in the field of solar energy and especially in environmental treatment because of their strong photocatalytic properties and chemical stability (Amin et al., 2009, Guo et al., 2009). However, TiO_2 has a large band - gap energy that requires ultraviolet irradiation to stimulate the catalytic ability. Furthermore, the rapid recombination of electron - hole pairs can drastically reduce quantum efficiency. So, narrowing the band - gap energy of TiO_2 to increase the visible light absorption ability is a commonly used method to improve photocatalytic efficiency (Amin et al., 2009). Such methods could be the addition of metals, metal oxides, various elements into TiO_2 lattice such as Zn, Fe, Cr, Eu, Y, Ag, Ni; or the insertion of nonmetals such as N, C, S, F, Cl; or simultaneously insertion of different elements into the TiO_2 crystal lattice, etc. Most of the modified products have higher catalytic activity than the initial TiO_2 in the visible light (Cotolan et al., 2016). Among them, silver is one of the most highly efficient ingredients (Guo et al., 2009; H. Dong et al., 2015). Over the years, the use of silver deposited on semiconductors in the photocatalytic process has much interest (for example, in the degradation of organic pollutants, hydrogen production, disinfection) because it can enhance the photocatalytic activity and extend the light absorption to the visible light region (Oros - Ruiz et al., 2013; Grabowska et al., 2013; Shan et al., 2008; Ansari et al., 2013; Khan et al., 2013). Silver, like other noble metals, acts as a trap of photogenerated electrons and as a result, improves the charge carrier separation (Ohtani et al., 1997). Moreover, silver nanoparticles can absorb visible light due to localized surface plasmon resonance (Zhou et al., 2012), leading to new applications such as antibacterial textiles, medical devices, food preparation surfaces as well as air conditioning filters and coated sanitary wares (Zielińska et al., 2010).

Currently, the combination of TiO_2 nanoparticles with halloysite nanotubes has been done by scientists with varied methods, and the results are promising. A typical example of this combination is Halloysite - TiO_2 composite photocatalytic material, which has a much higher decomposition rate for azo Basic Blue 41 dye in water than commercial TiO_2 under UV light (Szczepanik et al., 2017).

For that reason, the aim of this study is to fabricate a photocatalytic material based on HNT carrier with Ag - doped TiO_2 and to evaluate the activity of this catalyst in the photocatalytic degradation of RR - 195, which is a persistent pollutant present in textile wastewater.

2. Experimental

2.1. Chemicals

Raw halloysite was obtained from kaolinite mines. Sulfuric acid (H_2SO_4, 98%); Ethanol (C_2H_5OH); Acetic acid (CH_3COOH, 99%); Titanium iso - propoxide (TTIP) ($Ti(OC_3H_7)_4$); Silver nitrate ($AgNO_3$); Glucose ($C_6H_{12}O_6$); NH_3 solution; Hydroperoxide (H_2O_2); Reactive Red - 195 (RR195) were purchased from China; Deionized water and ice were produced directly at the lab and used throughout. All the chemicals were used without any further purification (except raw halloysite).

2.2. Halloysite (HNT) purification

Raw halloysite was crushed and sieved to remove particles and dried at 100^0C, then 40 g of the material was dissolved with 55 ml of distilled water. After that, a solution of 2 ml of 98% sulfuric acid was slowly added and stirred slowly at 90^0C for 90 minutes to obtain solution 1. This solution was filtered and washed several times with distilled water to remove excess H_2SO_4 and was

dried then. Next, 1.5 litters of distilled water were added to the mixture that has just been dried in previous step. The mixture was stirred for 24 hours more to acquire solution 2. Solution 2 was settled down for 96 hours and followed by a filtration. At this step, the upper part of solution 2 was decanted and, the residues at the bottom of the beaker were discarded. These separations were repeated 3 times. Finally, pure halloysite was obtained via the centrifugation, filtration and drying.

2.3. Synthesis of Ag - TiO_2, TiO_2 - HNT, Ag - TiO_2/HNT

First, 3.3 ml of CH_3COOH was cooled down in ice until completely frozen. Then, 6.6 ml of C_2H_5OH was added and stirred for about 30 minutes to obtain a completely transparent solution. TTIP (3.3 ml) was added to the solution and under magnetic stirring for 30 minutes. Then slowly added 280 ml of distilled H_2O to the solution, stirring for about 30 minutes, to obtain TiO_2 sol. Next, 3 g of purified halloysite was put to TiO_2 sol, and stirred at 65^0C for 24 hours, then kept it in an autoclave for 5 hours at 180^0C. The final solution was filtered, washed, and dried at 70^0C to TiO_2 - HNT.

Repeat the procedure until the step of TTIP addition. After that, 0.1 g of glucose was added under mild stirring, and the solution was heated up to 80^0C for 45 minutes.

In the following step, a solution of $AgNO_3$ 0.002M in excess NH_3 was added into the previous solution under hard stirring for 15 minutes to obtain sol Ag - TiO_2. After overnight aging, the gel was washed with acetonitrile repeatedly, vacuum - dried at 80^0C, and calcined in air at 550^0C for 2 h to produce Ag/TiO_2 powders.

To synthesize Ag - TiO_2/HNT, the sol was gradually cooled down to 65^0C with the addition of 3g of purified halloysite under normal stirring for 24 hours. The sol was kept at 180^0C in an autoclave for 5 hours. Finally, the solution was washed several times with filtration, then dried at 70^0C to obtain Ag - TiO_2/HNT.

2.4. Characterization

The phase structure of fabricated products was characterized by X - ray diffraction (Bruker, D8 advance) using CuK_λ (λ= 0.15406 nm) radiation. The data were collected in the range of $2\theta = 5^0$C to $2\theta = 80^0$C. Nitrogen adsorption analyses were carried out on Micromeritics ASAP 2000 at - 196^0C. All the samples were outgassed at 150^0C under vacuum for 1 hour prior to the measurements. Pore size distributions were determined using the BJH method from desorption branches of the isotherms. EDX spectra was recorded by EDS JED - 2300 Analysis Station. UV - vis spectra was obtained using Shimadzu UV - 3101 PC in the ultraviolet region in the wavelength range of 200÷800 nm. Transmission electron microscopy (TEM) was observed by a JOEL JEM - 1010 Electron Microsope while scanning electron microscope was taken by Philips XL30 microscope.

2.5. Measurement of photocatalytic activity

The photocatalytic activity was evaluated through the photocatalytic degradation of RR - 195. The efficiency of this reaction is calculated by determining the concentration of the dye before and after the reaction by UV - vis ultraviolet spectroscopy. Specifically, the concentration of RR - 195 was determined through the optical density obtained from ultraviolet spectroscopy at 541 nm. The efficiency of the degradation process is calculated by the following formula:

$$H\ (\%) = (C_o - C_t)/C_o \quad (1)$$

In which: C_o - initial concentration of RR - 195 (ppm); C_t - concentration of RR - 195 (ppm) after t (mins).

All the concentrations were identified based on calibration curves obtained by UV - vis.

3. Results and discussions

3.1. Characterization of purified HNT material

3.1.1. X - ray diffraction results

To determine the crystallographic structure of purified halloysite material, the *X* - ray diffraction spectrum was performed in the range 2θ from 5^0C to 80^0C. The XRD results of halloysite material are shown in Figure 1.

Wide - angle *X* - ray spectra of the purified halloysite sample show the appearance of characteristic peaks of halloysite nanotubes, in which the typical reflectance angles are at 2θ at 12.20 (001); 19.90 (100); 24.840 (002); 35.020 (110); 37.980 (003) and 54.340 (211) are

consistent with standard *X* - ray diffraction data of halloysite (HNT) nanotubes (Kamble et al., 2012).

3.1.2. SEM images of purified HNT

To determine the specific surface morphology for the purified halloysite material, the SEM method was conducted, and the scanning electron microscopy (SEM) image was obtained as shown in Figure 2.

The SEM image reveals that most of the purified halloysite has the form of tubes in nano size with porous structure and high uniformity.

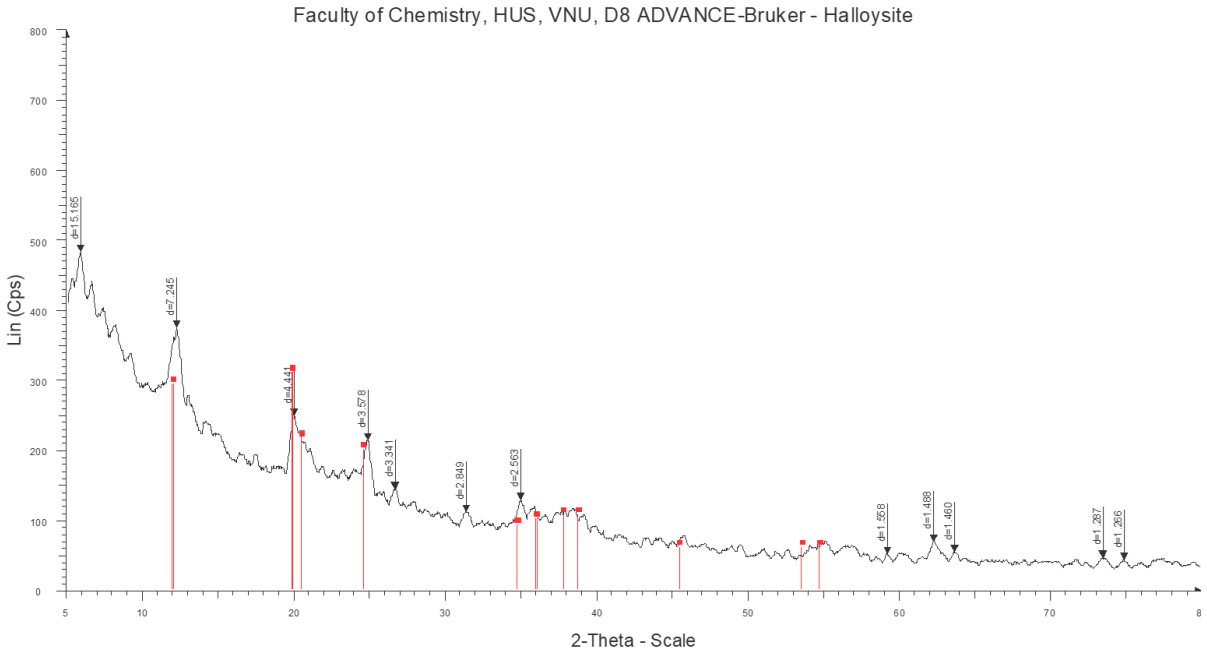

Figure 1. X - ray patterns (XRD) of purified halloysite.

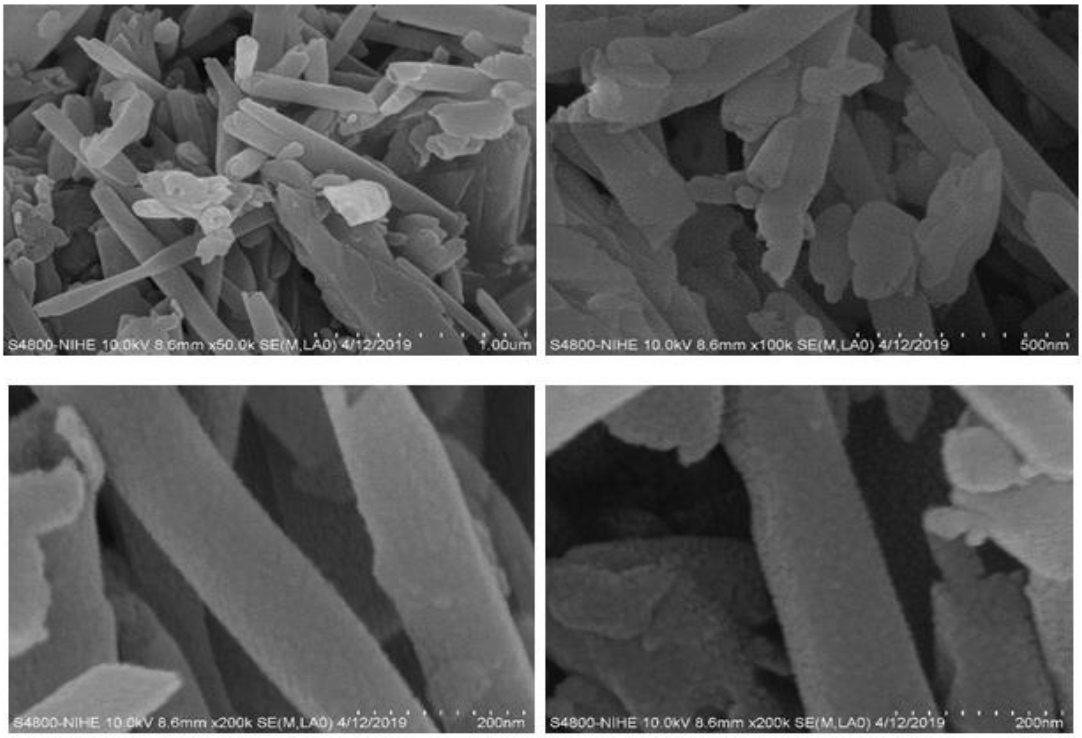

Figure 2. SEM images of purified Halloysite.

Specifically, the length of the tubes is about 1.3 µm, and diameter is about 130 nm, which is in accordance with results published in the literature (Rooj et al., 2010). The above results prove that halloysite (HNT) nanotubes have been successfully achieved from the raw halloysite source in Vietnam.

3.1.3. Nitrogen adsorption - desorption results

To determine the specific surface area and pore volume as well as pore diameter of HNT, the BET nitrogen adsorption - desorption isotherm at 77.3 K according was carried out for halloysite nanotube material samples.

The curves are exhibited in Figure 3, showing that the adsorption - desorption isothermal curve of the HNT is of type IV and has a hysteresis curve H3 corresponding to the mesoporous material according to IUPAC classification. The pore size distribution curve illustrates that the mean pore diameter of HNT was 4.8 nm.

Typical parameters of HNT obtained from BET measurement results:

- Specific surface area (S_{BET}): 28.0186 m^2/g
- Total pore volume (V_{pore}): 0.137840 cm^3/g
- Pore diameter (*DBJH*): 21.8489 nm.

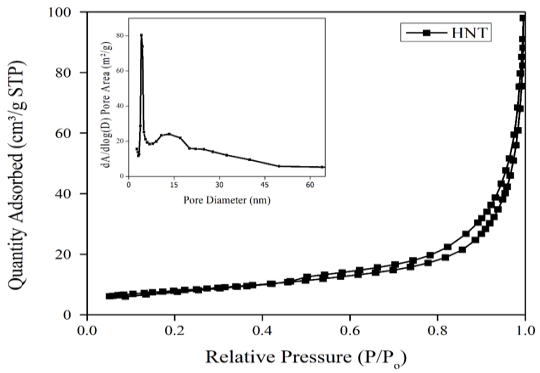

Figure 3. Nitrogen adsorption - desorption isotherm at 77.3 K of HNT.

3.1.4. Characterization of Ag - TiO_2/HNT

The results of XRD, UV - vis solid, EDX and SEM of Ag - TiO_2/HNT materials are exhibited in Figures 4÷7.

X - ray spectrum of Ag - TiO_2/HNT material (Figure 4) still confirms the existence of the characteristic peaks of TiO_2, which proves that there is no change in the structure of TiO_2 material.

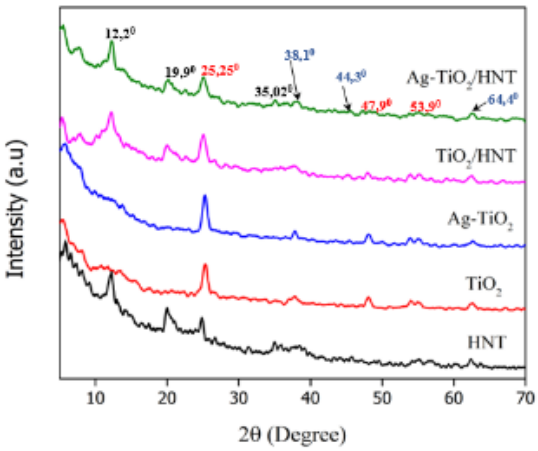

Figure 4. X - ray (XRD) spectrum of different catalysts.

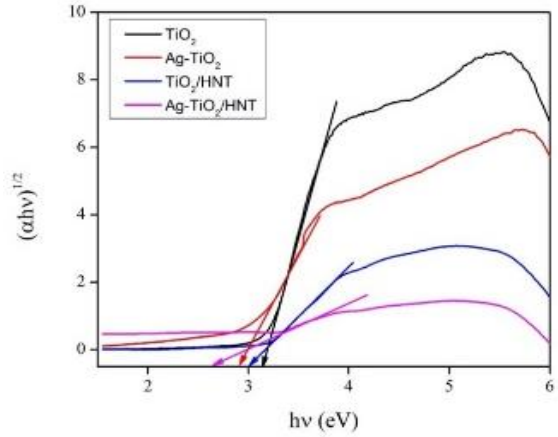

Figure 5. Graph of $[F(R)hv]^2$ as a function of hν for E_{bg} calculation.

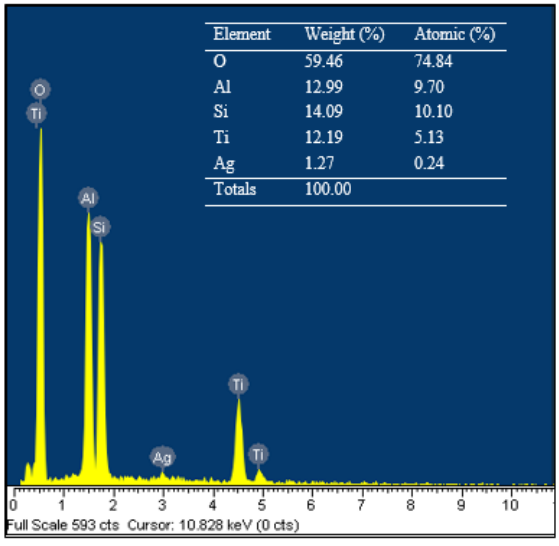

Figure 6. EDX spectrum of Ag - TiO_2/HNT.

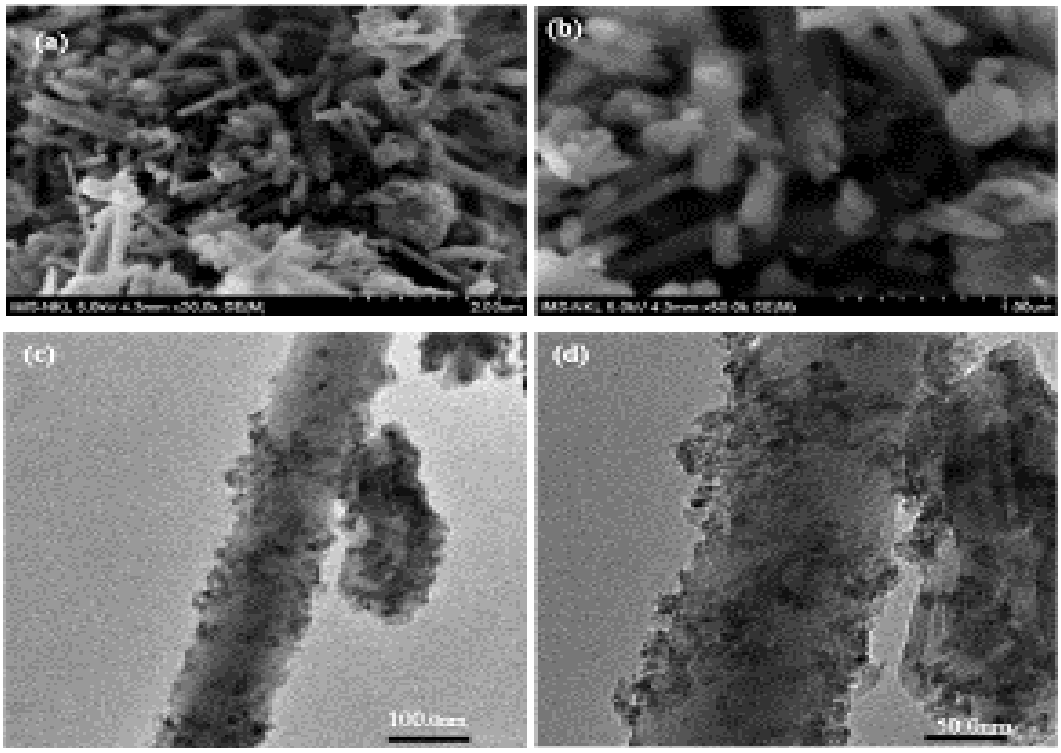

Figure 7. SEM (a and b), TEM (c and d) images of Ag - TiO_2/HNT.

There are additional peaks which appear at 2θ = 38.1 (111) and 64.4 (220) and weaker intensity peak at 2θ = 44.3 (200) characterizing the presence of metallic silver (JCPDS 65 - 2871). The obtained results demonstrate that the insertion of TiO_2 and Ag - TiO_2 on the HNT support causes no effect on the halloysite nanotube structure.

The band - gap energy Eg of the photocatalytic materials TiO_2, Ag - TiO_2, TiO_2 - HNT, Ag - TiO_2/HNT were 3.2 eV, 2.8 eV, 3.0 eV, and 2.6 eV, respectively that were indicated in Figure 5. Those values appear to verify that the combination of HNT and TiO_2 has adjusted the band - gap of TiO_2 3.2÷3 eV. Furthermore, the addition of Ag onto the surface of TiO_2 has drastically reduced the band - gap of TiO_2 to 2.8 eV that could consequently lead to a significant influence on the photocatalytic properties of TiO_2. Thereby, the excited zone of Ag - TiO_2/HNT shifted considerably from the ultraviolet (UV) to the visible (Vis) region, and the material has a narrower band - gap (2.6 eV) compared to pure TiO_2 (3.2 eV)

Also, the X - ray energy dispersive spectrum of Ag - TiO_2/HNT in the binding energy range of 0÷10 keV in Figure 6 points out the corresponding signals of the elements that make up the Ag - TiO_2/HNT catalyst and no different elements appear. Additionally, the mass percentage of the elements are quite compatible with the theoretical calculation used in the first step to synthesize Ag - TiO_2/HNT.

SEM, TEM images (Figure 7) presents that the implantation of Ag - TiO_2 onto halloysite nanotubes did not break the halloysite's tube structure. The images show the uniform dispersion of the Ag - TiO_2 nanoparticles on halloysite (HNT) nanotubes and the Ag nanoparticles that are tightly attached on the surface of the TiO_2 nanorods to form Ag - TiO_2 nanorods with an average size is about 10÷20 nm.

As can be described in Figure 8 and Table 1, Ag - TiO_2/HNT has twice as much specific surface area and significantly increased pore volume as the HNT support. It could be explained that Ag - TiO_2 also has its own specific surface area and has its porous system. As a result, the presence of Ag - TiO_2 on the inner and outer surface of halloysite nanotubes could contribute to the number of pores representing for the higher surface area as well as the total pore volume. The higher pore volume of Ag - TiO_2/HNT could guarantee the better performance of this catalyst in terms of pollutants

adsorption. Based on the evidence given by various characterization techniques, it could be concluded that Ag - TiO_2 was successfully grafted on the surface of HNT. Moreover, Ag - TiO_2 particles in nano size, which were distributed evenly on the surface, could bring efficient catalytic activity to the as - prepared nanocomposite.

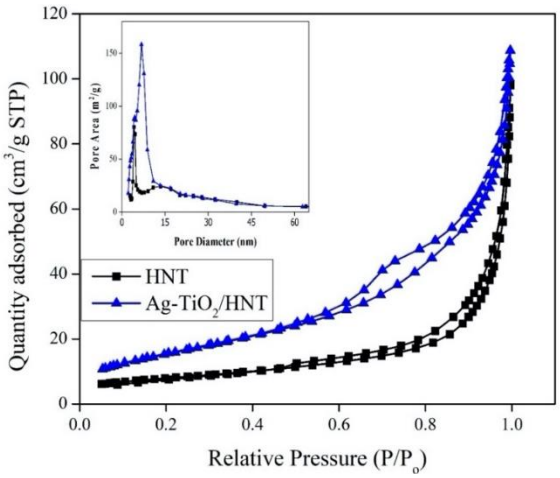

Figure 8. Nitrogen adsorption - desorption isotherm at 77.3K of Ag - TiO_2/HNT catalyst.

Table 1. Parameters of Ag - TiO_2 - HNT obtained from BET method.

Parameter	Value
Specific surface area (S_{BET} - m^2/ g)	57.3668
Pore diameter (D_{BJH} - nm)	10.6906
Pore volume (V_{pore} - cm^3/ g)	0.163701
Micropore volume (cm^3/ g)	0.000193

3.2. Photocatalytic activity of Ag - TiO_2/HNT

3.2.1. Comparison of photocatalytic activity of synthesized materials

The photocatalytic decomposition of RR - 195 was performed at room temperature with the following conditions: the initial concentration of RR - 195 in water was 50 ppm, then 1.5 ml of H_2O_2 was added with 0.05 g solid catalyst. Next, the mixture was stirred for 3 hours to reach equilibrium adsorption. After that, the mixture was irradiated with UV light for the next 3 hours. The results of the catalytic activity evaluation are presented in Figure 9.

The results pointed out that the Ag - TiO_2/HNT synthesized by the direct method has the highest photocatalytic activity. This can be elucidated by the existence of Ag - TiO_2 on the surface of halloysite reduced the band - gap energy of TiO_2 (2.6 eV). In addition, Ag^o can be a center of charge transition and has high ability to trap electrons to prevent recombination of photo - generated electrons and holes on TiO_2 surface. At the same time, silver also has a plasmon resonance effect resulting in the more OH radical generation and increased photocatalytic efficiency.

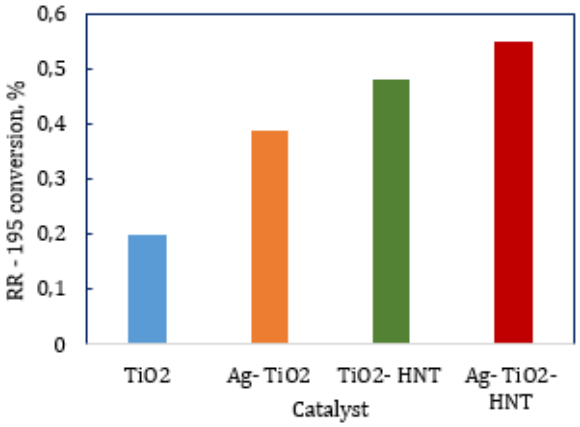

Figure 9. Conversion of RR - 195 in photocatalytic degradation process using different catalysts.

3.2.2. Impact of H_2O_2 concentration on the conversion of RR - 195

H_2O_2 has an important impact on the photocatalytic degradation of pollutants. The effect of H_2O_2 in RR - 195 was investigated, and the results are presented in Figure 10.

As can be observed in Figure 10, when using 2 ml of H_2O_2 with the presence of Ag - TiO_2/HNT catalyst under UV irradiation, the conversion of RR - 195 was 79% in a period of 360 minutes. When increasing the amount of H_2O_2 to 4ml, the mineralization of RR - 195 after 360 minutes did not occur faster but tended to decrease (76%). In addition, if the amount of H_2O_2 is reduced to 1ml and 1.5 ml, the rate as well as the decomposition efficiency RR - 195 decreased also standing at 66% and 76%, respectively.

This is because more •OH radicals generated from H_2O_2 promote the reaction leading to increased decomposition rate and efficiency. However, when the amount of H_2O_2 in the solution is too high or too low will reduce the free radicals •OH occurs according to the equation (Szczepanik

et al., 2017; Abdel Fattah et al., 2016; Natarajan et al., 2015):

$$H_2O_2 + \bullet OH \rightarrow \bullet HO_2 + H_2O$$
$$\bullet HO_2 + \bullet OH \rightarrow O_2 + H_2O \quad (2)$$

In addition, a high amount of H_2O_2 also results in the saturation of the active sites of the catalyst, thereby diminishing the reaction rate. For that reason, 1.5 ml of H_2O_2 was chosen to be applied to all remaining research processes to best assess the catalytic activity of the catalyst materials.

3.2.3. Influence of catalyst weight

The influence of the catalyst content on the conversion of dye RR - 195 on Ag - TiO_2/HNT catalyst was investigated. The results are shown in Figure 11.

The results showed that after 360 minutes of UV irradiation using 0.15 g of Ag - TiO_2/HNT, the efficiency in RR - 195 degradation was 96%. This value is considerably higher than the ones obtained when 0.05g and 0.1g catalyst was applied, which only reached the conversion of 66% and 90%, respectively. This can be explained as follows: when the amount of catalyst increases, the amount of catalytic activity sites increases, causing the diffusion rate of the anions RR - 195 to the active sites on the surface, leading to an increase the number of 96% shows the almost complete decomposition of contaminants under normal conditions.

4. Conclusions

This study has obtained some remarkable results with a relatively new photocatalytic material system based on the halloysite natural mineral. Specifically, purified halloysite (HNT) nanotubes have been processed from raw halloysite sources in kaolin mines in a specific surface area of 28.0186 m^2/g with an average length of 1.3 µm and average diameter of 130 nm. Ag - TiO_2/HNT photocatalytic material was then synthesized by the direct method. The data showed that the doping of Ag significantly narrowed the band - gap energy of pure TiO_2. Thus, the material could be easily excited in the visible region, which makes it more efficient in the photocatalytic process. In addition, the specific area and pore volume of Ag - TiO_2/HNT were significantly improved in comparison with HNT and TiO_2. The photocatalytic activity evaluation indicated that the Ag - TiO_2/HNT had superior efficiency compared to the other catalysts namely TiO_2; Ag - TiO_2; TiO_2/HNT thanks to the presence of Ag and the better distribution of active phase on HNT support. As a result, Ag - TiO_2/HNT could almost completely decomposed RR - 195 at room temperature and neutral pH environment. This suggests that Ag - TiO_2/HNT material could offer extreme potential in the treatment of polluted wastewater.

Author contributions

Son Ha Ngo and Nui Xuan Pham conceived and planned the experiments; Tuan Ngoc Tran carried out the experiments; Son Ha Ngo and Tuan Ngoc Tran contributed to sample preparation. Son Ha Ngo and Nui Xuan Pham contributed to the interpretation of the results; Son Ha Ngo and Tuan

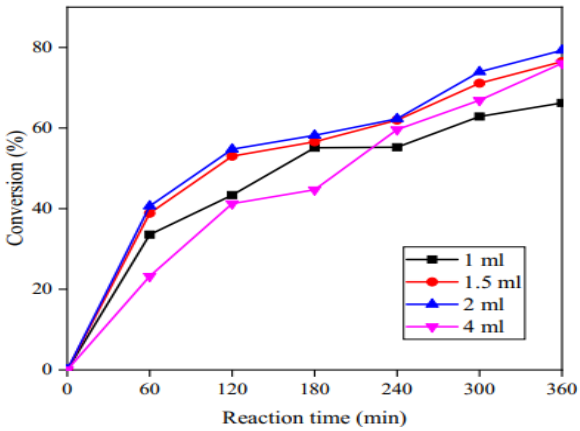

Figure 10. The conversion of RR - 195 when using Ag - TiO_2/HNT at different H_2O_2 concentrations.

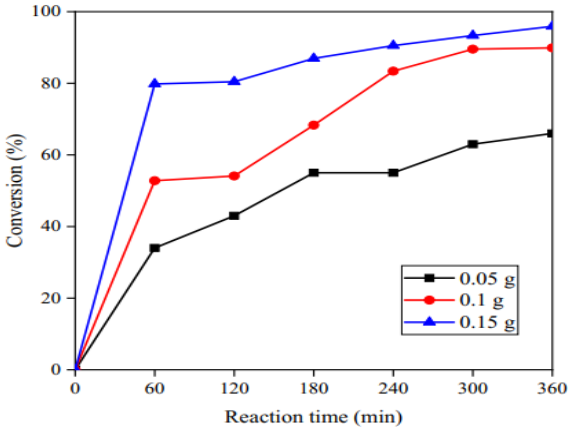

Figure 11. Influence of catalyst weight in the degradation process of RR - 195.

Ngoc Tran performed the calculations; Son Ha Ngo took the lead in writing the manuscript. All authors provided critical feedback and helped shape the research, analysis and manuscript.

References

Ansari, S. A., Khan, M. M., Ansari, M. O., Lee, J. & Cho, M. H. (2013). Biogenic synthesis, photocatalytic, and photoelectrochemical performance of Ag - ZnO nanocomposite. *J. Phys. Chem. C., 117*, 27023 - 27030.

B. Szczepanik, P. Rogala, P.M. Słomkiewicz, D. Banaś, A. Kubala - Kukuś, I. Stabrawa. (2017). Synthesis, characterization and photocatalytic activity of TiO_2 - halloysite and Fe_2O_3 -halloysite nanocomposites for photodegradation of chloroanilines in water, *Appl. Clay Sci., 149,* 118 - 126.

G. Guo, B. Yu, P. Yu, X. Chen. (2009). Synthesis and photocatalytic applications of Ag/TiO_2 -nanotubes. *Talanta, 79,* 570 - 575.

Grabowska, E., Zaleska, A., Sorgues, S., Kunst, M., Etcheberry, A., Colbeau - Justin, C., Remita, H. (2013). Modification of titanium (IV) dioxide with small silver nanoparticles: application in photocatalysis. *J. Phys. Chem. C., 117,* 1955 - 1962.

H. Dong, Zeng, Tang, . Fan, Zhang, He, H. (2015). An overview on limitations of TiO_2 - based particles for photocatalytic degradation of organic pollutants and the corresponding countermeasures, *Water Res., 79,* 128 - 146.

K. Imamura, E. Ikeda, T. Nagayasu, T. Sakiyama, K. Nakanishi. (2002). Adsorption behavior of methylene blue and its congeners on a stainless steel surface. *J. Colloid Interface Sci., 245*, 50 - 57.

Khan, M. M., Ansari, S. A., Amal, M. I., Lee, J. & Cho, M. H. (2013). Highly visible light active Ag/TiO_2 nanocomposites synthesized using an electrochemically active biofilm: a novel biogenic approach. *Nanoscale, 5,* 4427 - 4435.

N. Cotolan, M. Rak, M. Bele, A. Cör, L.M. Muresan, I. Milošev. (2016). Sol - gel synthesis, characterization and properties of TiO_2 and Ag - TiO_2 coatings on titanium substrate. *Surf. Coatings Technol. A., 307,* 790 - 799.

Ohtani, B., Iwai, K., Nishimoto, S. & Sato, S., (1997). Role of platinum deposits on titanium (IV) oxide particles: structural and kinetic analyses of photocatalytic reaction in aqueous alcohol and amino acid solutions. *J. Phys. Chem. B 101,* 3349 - 3359.

Oros - Ruiz, S., Zanella, R., López, R., Hernández - Gordillo, A. & Gómez, R., (2013). Photocatalytic hydrogen production by water/methanol decomposition using Au/TiO_2 prepared by deposition - precipitation with urea. *J. Hazard. Mater. 263,* 2 - 10.

R. Kamble, M. Ghag, S. Gaikawad, B. Panda, 2012. Halloysite Nanotubes and Applications: A Review. *J. Adv. Sci. Res. 3,* 25 - 29.

S. Bagane, M., Guiza, (2000). Removal of a dye from textile effluents by adsorption. *Ann. Chim. Sci. Mater 25,* 615 - 626.

S. M., K. Natarajan, (2015). Antibiofilm Activity of Epoxy/Ag - TiO_2 Polymer Nanocomposite Coatings against Staphylococcus Aureus and Escherichia Coli. *Coatings. 5 (2),* 95 - 114.

S. Rooj, A. Das, V. Thakur, R.N. Mahaling, A.K. Bhowmick, G. Heinrich, (2010). *Preparation and properties of natural nanocomposites based on natural rubber and naturally occurring halloysite nanotubes.* Mater. Des. 31, 2151 - 2156

S. A. Amin, M. Pazouki, A. Hosseinnia, (2009). Synthesis of TiO_2 - Ag nanocomposite with sol - gel method and investigation of its antibacterial activity against E. coli. *Powder Technol*., 196, 241 - 245.

Shan, Z., Wu, J., Xu, F., Huang, F. - Q. & Ding, H., (2008). Highly effective silver/semiconductor photocatalytic composites prepared by a silver mirror reaction. *J. Phys. Chem. C 112,* 15423 - 15428.

W.I. Abdel Fattah, M.M. Gobara, W. El - Hotaby, S.F.M. Mostafa, G.W. Ali, (2016). Coating stainless steel plates with Ag/TiO_2 for chlorpyrifos decontamination. *Mater. Res. Express. 3 (5).*

Y. Zhang, A. Tang, H. Yang, J. Ouyang. (2016). Applications and interfaces of halloysite nanocomposites. *Appl. Clay Sci., 119,* 8 - 17.

Zhou, X., Liu, G., Yu, J. & Fan, W. Surface plasmon resonance - mediated photocatalysis by noble metal - based composites under visible light. *J. Mater. Chem*., *22*, 21337 - 21354 (2012).

Zielińska, A., Kowalska, E., Sobczak, J. W., Łącka, I., Gazda, M., Ohtani, B., Hupka, J., Zaleska, A. (2010), Silver - doped TiO_2 prepared by microemulsion method: surface properties, bio - and photoactivity. Sep. *Purif*. *Technol*., 72, 309 - 318.